

UNIVERSITY OF CALIFORNIA,  
IRVINE

Design and Fatigue Evaluation of Parameters for Crack Detection: An in  
Vitro Study

THESIS

submitted in partial fulfillment of the requirements  
for the degree of

MASTER OF SCIENCE

in Biomedical Engineering

by

Parsa Zamani Mazdeh

Thesis Committee:

Professor James C. Earthman, Chair  
Assistant Professor Michelle Digman  
Professor William Tang

2019



# TABLE OF CONTENTS:

<b>LIST OF FIGURES .....</b>	<b>iii</b>
<b>LIST OF TABLES .....</b>	<b>iv</b>
<b>ACKNOWLEDGMENTS .....</b>	<b>v</b>
<b>ABSTRACT .....</b>	<b>vi</b>
<b>CHAPTER 1: Introduction.....</b>	<b>1</b>
1.1 Background .....	1
1.1.1 Fracture resistance mechanics.....	1
1.1.2 Fracture resistance of tooth tissues .....	2
1.1.3 Evaluation of fatigue properties/behaviour.....	3
1.1.4 Current diagnostic tools for cracked tooth.....	3
1.2 Research Aims.....	5
1.3 Significance.....	5
<b>CHAPTER 2: Materials &amp; Methods .....</b>	<b>6</b>
2.1 Sample selection.....	6
2.2 Methodology .....	6
2.2.1 Fatigue cyclic machine testing.....	7
2.2.2 Quantitative percussion testing .....	8
2.2.3 Fracture surface examination.....	11
2.3 Statistical analysis .....	11
<b>CHAPTER 3: Results &amp; Discussion.....</b>	<b>13</b>
3.1 Fatigue cycling and Crack initiation .....	13
3.1.1 Summary of findings.....	13
3.1.2 Pilot fatigue testing of simulated teeth.....	14
3.1.3 Experimental fatigue testing of simulated 3D teeth.....	14
3.2 Significance of findings and clinical implications .....	17
3.3 Limitations of the study.....	17
3.4 Conclusions and Future directions .....	18
<b>REFERENCES.....</b>	<b>20</b>
<b>APPENDIX A: Load data for simulated 3D teeth .....</b>	<b>23</b>
<b>APPENDIX B: Fatigue Testing Procedure.....</b>	<b>25</b>

## LIST OF FIGURES:

Figure 1. Setup of loading device. ....	6
Figure 2. Fatigue machine used in the present research. ....	7
Figure 3. Periometer system .....	9
Figure 4. QPD generated energy return graphs .....	10
Figure 5.. SEM of the Cross-section of 3D simulated teeth. ....	12
Figure 6. Examples of simulated teeth.....	15
Figure 7. Fatigue test in experimental simulated models .....	16
Figure 8. Fatigue testing plot .....	19

## LIST OF TABLES:

Table 1. Crack detection within simulated 3D tooth specimens determined by QPD technology.....	13
Table 2. Paired Samples Statistics for 3D tooth numbers 6 and 7.....	14

## **ACKNOWLEDGMENTS**

I like to acknowledge the assistance of several people without whom this project would not have been possible. First and foremost, my deepest gratitude to my supervisor Dr. Earthman for his unwavering support and mentorship throughout this project. He has shown immense patience to answer all my questions and guide me to achieve the goals of this research project. I also wish to extend my appreciation to the laboratory technician Mr. Ching Hao who assisted in setting up the experiments and collection of data for this project. Last but not least my gratitude goes to my committee members Dr. Tang and Dr. Digman for their precious time and commitment.

## **ABSTRACT**

By

Parsa Zamani

Master of Science in Biomedical Engineering

University of California, Irvine, 2019

Professor James C. Earthman, Chair

Understanding fatigue is important to the success of dental materials as evident from the eventual failure of restorations and cyclic loads during mastication. However, detection of such failures often poses clinical challenges as most cracks are invisible or subsurface when initiated and only identified when catastrophic failures occur. Current detection methods are limited in clinical application. Therefore, the aim of this research study was to design a test method and parameters that simulate the oral environment to assess the detection of crack initiation and growth using quantitative percussion diagnostics (QPD) technology. Nine 3D tooth models were subjected to cyclic fatigue loading amplitudes of 92 N accompanied by periodic QPD testing. Normal fit error values determined by QPD before loading and after fatigue cycling testing were recorded for the 3D simulated teeth. Results showed that location and depth of notch were important determinants of the number of cycles to crack initiation. The QPD device was able to monitor crack initiation and growth in at least three of the simulated teeth with accuracy. Although each tooth was found to reach failure at a different cycle number, the paired comparison was non-significant ( $p= 0.099$ ) indicating results are comparable. Future analysis requires more simulated teeth to confirm these findings. Also, a comparison of the data obtained from 3D tooth models to natural extracted teeth as well as comparison to existing diagnostic tools used for crack identification would be warranted. These preliminary findings provide further evidence for the use of QPD as a diagnostic aid for early crack identification and monitoring structural integrity of teeth.

# CHAPTER 1: Introduction

---

## 1.1 Background

Teeth are load-bearing structures capable of withstanding significant masticatory load (>700N). Progressive mechanical degradation results in fatigue leading to tooth fracture and one of the major contributors to tooth failure. Therefore, in recent years more attention has focused on improving methods and technologies for prediction of failures due to hard tissue flaws or fractures.<sup>1,2</sup>

### *1.1.1 Fracture resistance mechanics*

The basic hard tissue components of teeth are composed of the crown and root structures. The tooth crown consists of enamel as the highly mineralized outermost layer enclosing dentin which has less mineral content and serves as a protective layer for the dental pulp. The root located beneath the crown part also mostly consists of dentin with a thin cementum layer connecting tooth and alveolar bone via the periodontal ligament.

Recent interest in the capacity of teeth to withstand heavy masticatory loads and maintain oral function has led to the development of empirical models to predict a range of loads for initiation of crack that leads to tooth failure<sup>3</sup> ( see review by Lawn & Lee 2009). Yahyazadehfar et al.<sup>4</sup> describes the longitudinal and margin cracks as the two main types of crack under load. They further divide longitudinal cracks to radial and median cracks which initiate from the enamel base extending to the surface and ‘shear-nucleated’ flaws starting under the contact load zone extending apical of the enamel, respectively.<sup>4</sup> On the other hand, margin cracks form at the dentin-enamel junction (DEJ) from inherent flaws and travel towards occlusal surface. Other factors contribute to the failure of teeth include dietary habits, tooth morphology, and tooth size.<sup>5</sup>



Research indicates at least 200N contact load is required for margin cracks with a range of 400-600 N resulting propagation towards occlusal surfaces and longitudinal cracks requiring much higher load ranges.<sup>4</sup>

There are essentially two main properties that govern fracture in natural teeth: fracture toughness and the ability of dental tissue to resist fatigue crack growth. Generally, for fracture toughness measurements bending notched or compact tension specimens are used to generate cracks which grow with increased application of tensile stress.<sup>6</sup>

### ***1.1.2 Fracture resistance of tooth tissues***

Both dentin and enamel exhibit a large variation in fracture resistance due to primarily differences in biomechanical properties, reported the difference in microstructure, experimental conditions, structural anisotropy, oral environment, and the aging process.<sup>4</sup> Specifically, variation in enamel fracture toughness (0.7 to 1.3 MPa m<sup>1/2</sup>) is due to prism orientation with cracks extending parallel to the enamel rods. Over long periods, the growth of small cracks on the outer surface may lead to mechanical breakdown or demineralization.<sup>7</sup> Dentin has a complex microstructure with a unique tubular architecture enclosed by random apatite crystallites. Dentin fracture toughness varies between 1.0 to 2.0 MPa m<sup>1/2</sup> as cracks grow in various directions. One toughening mechanism that contributes to hard tissue crack growth resistance has been proposed as the DEJ providing a barrier to crack propagation through the bridging mechanism.<sup>8</sup> The DEJ region reportedly prevents enamel cracks to traverse the interface due to the presence of ligament bridging.<sup>8</sup> In dentin, bridging of the uncracked ligament (thin areas of unbroken material) acts by supporting part of the applied load thereby reducing 'crack-driving force' and preventing crack propagation.<sup>8</sup>

### ***1.1.3 Evaluation of fatigue properties/behavior***

Several methods have been investigated to evaluate the fatigue properties of dental hard tissues as well as restorative materials. Some of these approaches include compact sandwich specimen, a notchless triangular prism (NTP) developed to evaluate fracture durability of biomaterials and hard tissues<sup>9</sup> and compact tension (CT) evaluation of hard tissue properties as well as a crack extension under fatigue load. However, the CT configuration can only be applied to studies of coronal dentin due to limitations of tissue volume.<sup>4</sup>

Other problems with evaluation of teeth fatigue properties is accurate preparation of specimen due to small size and unintended mixed loading which can occur in biomaterials due to oblique propagation of cracks in flexural configurations.<sup>4</sup> While earlier investigations of enamel fracture resistance involved indentation methods as they do not need a pre-crack for evaluation and simple to perform on smaller volumes of brittle materials, however, a large number of models for measurement of fracture toughness have given inaccurate characterization results compared to other methods, which has limited the use of the indentation approach.<sup>4</sup> To overcome restricted material volume reported with conventional approach, a miniature inset CT configuration of 2 mm whereby the hard tissue is molded within a resin, has been found practical for evaluation of fracture properties of biomaterials with small volumes.<sup>10</sup>

### ***1.1.4 Current diagnostic tools for a cracked tooth***

The traditional diagnostic tools for identification of cracked tooth are based on patient symptoms, special dyes, bite tests and visual clinical examination. These conventional aids although useful in some cases, mostly have shortcomings in accurate clinical diagnosis of dental cracks.

Although dental history such as clenching, pain on biting and thermal sensitivity can provide some clinical clues, a definitive diagnosis can be challenging since the pain may be referred

pain or mimic other oral pathologies such as sinusitis.<sup>11</sup> When the fracture extends gingivally a periodontal probe might be useful. However, a deep probe pocket may indicate a split tooth rather than a simple fracture line. Methylene blue dyes can be useful to emphasize a fracture line.<sup>11</sup> However, some external cracks or incomplete fracture lines do not readily accept the dye.<sup>12</sup>

Other diagnostic tools include bite tests, transillumination, microscopic visualization, and ultrasound techniques. Bite tests are one of the most common diagnostic tools used in dentistry and can be performed using cotton wool rolls, wood sticks or commercial tools such as Fractfinder and Tooth Slooth to isolate a fractured cusp. In recent years, the use of a clinical microscope has been advocated for evaluation of early enamel cracks but visualization of the crack requires the tooth to be thoroughly cleaned, significant operational experience and clinical skills for an accurate diagnosis.<sup>12</sup> Also, ultrasound imaging has been shown to detect planar cracks based on its shorter wavelength and high-resolution capacity. However, the clinical application of ultrasound is restricted owing to the complex micro-anatomic structure of natural teeth with an outer surface that is often curved.<sup>13</sup>

When using transillumination, the tooth needs to be clean and plaque-free to be able to directly place the light on the tooth. The drawback is that transillumination can only be used to detect wide open structural cracks and is unable to locate any subtle changes resulting from fine cracks. Newer imaging techniques such as near-IR transillumination imaging takes advantage of enamel transparency by using optical coherence tomography (OCT) to acquire images of internal cracks formed and propagated in teeth.<sup>14</sup> These technologies are currently expensive, require expertise and are difficult to use in clinical settings.

In summary, cracks in teeth can propagate based on the fatigue properties of enamel and dentin. In addition, aging and acidic oral environment reduce enamel and dentin tolerance towards this

insult. The present research is designed to design and develop parameters for a cyclic fatigue machine that allows investigating the detection of cracks using quantitative percussion diagnostics (QPD) in a laboratory setting.

## **1.2 Research Aims**

The primary aim of this research study is to induce and detect crack initiation in tooth simulate samples as well as extracted teeth using a novel cyclic fatigue device and quantitate cyclic crack growth. Furthermore, to design and develop a cyclic fatigue device for easy and efficient detection of dental hard tissue fatigue. The results will provide a better understanding of fatigue properties of teeth as well as assess the capabilities of QPD for determining size and location of cracks in teeth.

## **1.3 Significance**

Cracks in hard tissue tend to occur either in coronal or root structure and need to be identified early on to treat and prevent further growth. Despite the extensive research completed on fatigue failure of dental tissues and a number of different strategies employed to detect cracks in teeth, current diagnostic aids have clinical limitations and no single method has been reported to detect initiation and growth of cracks in dental hard tissues accurately. The idea behind this research work is to design and plan an experimental fatigue test machine suitable for measuring cracks in teeth. It is hoped that the outcomes of this research will further our understanding of fatigue properties of teeth which is also indirectly relevant to developing novel dental materials with improved fracture resistance.

## CHAPTER 2: Materials & Methods

---

### 2.1 Sample selection

The fatigue testing specimens for this study were selected from fabricated synthetic teeth which are accurate 3-dimensional (3D) replicas of natural teeth (TruTooth; DeLendo). These synthetic 3D teeth models are dimensionally stable with comparable material characteristics to that of natural teeth. The material consists of a transparent polymer (VeroClear-RGD810) that is rigid to replicate complex anatomy of a tooth in detail. Nine of these synthetic models were used instead of extracted teeth as almost all-natural teeth have some degree of damage due to extraction procedure making accurate and consistent data collection very challenging.

### 2.2 Methodology

The nine synthetic 3D teeth were consecutively numbered. We used four of the 3D replicas out of nine molar teeth to pilot test the experiment. Each 3D tooth model was inserted in an acrylic resin housing (Figure 1a). The specimen holder was labeled Buccal (B), Lingual (L), Mesial (M), and Distal (D), with the test conducted involving the M-B and D-L cusps of the simulated tooth (Figure 1b)

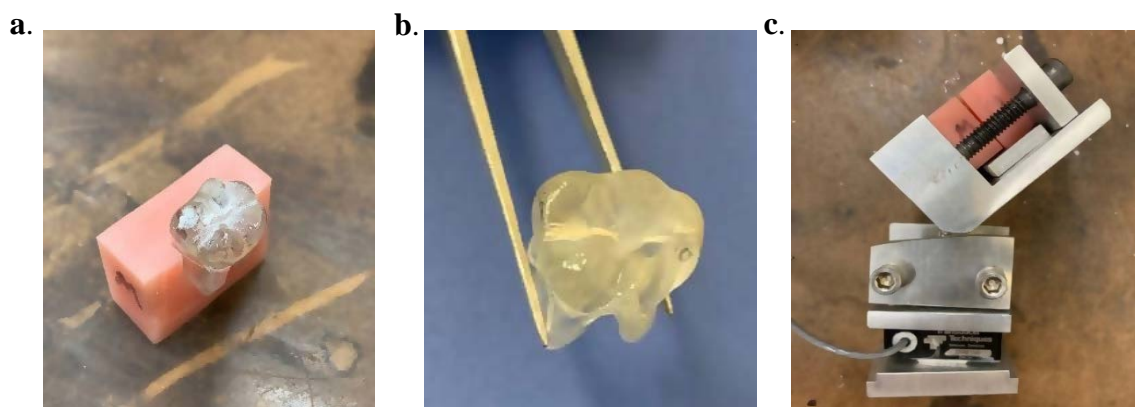


**Figure 1. Setup of loading device.** a. Simulated tooth embedded in acrylic resin housing. b. 3D printed simulated molar tooth. c. Load cell assembly with simulated tooth secured in resin housing. Range of measurement is recorded between 23-115 Newton.

The simulated tooth was then secured by two screws in the stainless-steel holder at a 45-degree angle to the load cell assembly (Model MLP 50), simulating tooth position in the oral cavity (Figure 1c). We used a force in the range of 92-115 N, while the load cell is capable of measuring forces of up to 222 N.

### ***2.2.1 Fatigue cyclic machine testing***

Fatigue tests were carried out using a custom-made fatigue testing machine (Edward Life Science CA, US) with a unidirectional load pressing the cusp of the simulated tooth at a 45-degree angle (Figure 2). Once the simulated tooth is assembled onto the loading cell, the assembly is inserted into the loading section of the fatigue machine (Figure 2A). We used the adjustable speed motor at a high frequency of 34 cycles per second for each test (Figure 2B). The same tooth sample was tested again at increasing stress level until failure which was defined as either loosening or fracture of the simulated tooth assembly. All tests were performed at room temperature.

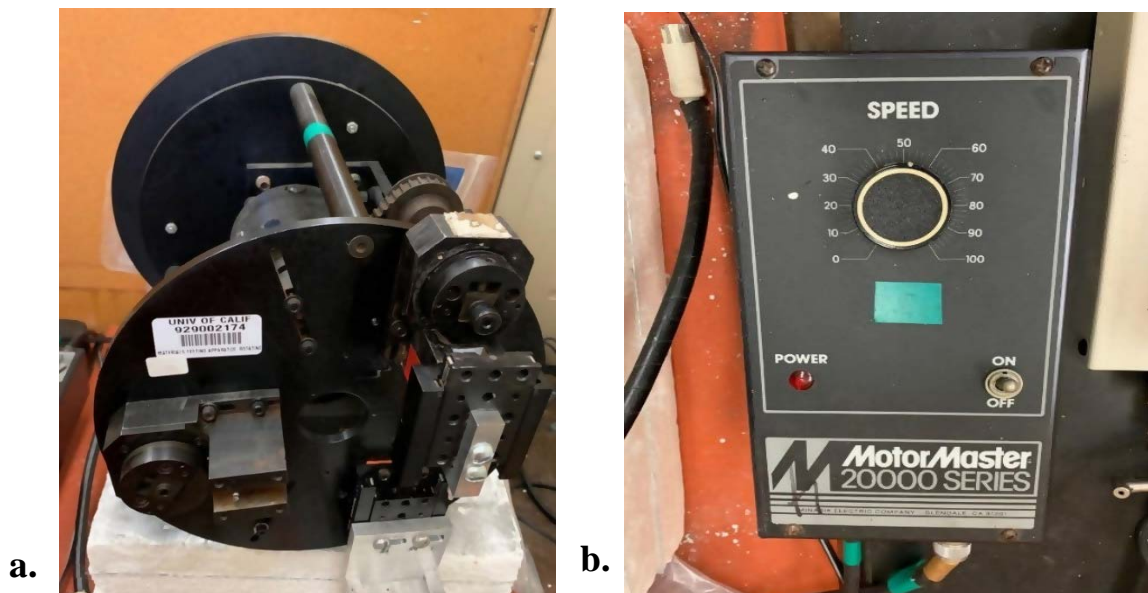


**Figure 2. Fatigue machine used in the present research. a.** The load cell-tooth assembly is inserted here and secured the fatigue machine. **b.** Adjustable speed motor used to control the frequency of testing.

The simulated tooth sample cusp position is determined by the action of Motion Controller (Newport Co, US) which generates power to move the actuator device with an accuracy of 0.00001 meters resulting in vertical movement of the tooth sample.

After the fatigue machine is set up and tooth assembly loaded, custom LabVIEW software was used to set the required parameters for conducting the testing (Appendix B). This software allows setting of the desired frequency and load amplitude. Once the weight of the chamber (housing the simulated tooth) is entered then the minimum and maximum forces are manually adjusted through fatigue machine. This adjustment is performed via the rotation of a cylindrical disk to ensure no gap is formed between the pin and cusp of the simulated tooth. In order to accelerate crack formation an R ratio of 0.2 was applied for specimen 4 to 9. The simulated tooth was tested using QPD every 10k cycles up to 100k cycles initially followed by every 5k cycles up to 130k cycles and finally every 3k cycles until the tooth showed signs of crack formation.

### ***2.2.2 Quantitative percussion testing***

#### **Quantitative Percussion Diagnostic**

The fatigue machine was automatically stopped after 10k cycles to check the specimen for potential cracks using Quantitative Percussion Diagnostic (QPD) technology (Periometer®, Perimetrics, LLC). This machine was originally developed for recording and assessing percussion response of human teeth and dental implants.<sup>15,16</sup> The QPD components include a custom computer software interfaced to a percussion probe and a control unit instrument to capture data and allow analysis together with the visualization of outcomes. The probe transmits vibrations in the tooth structure and the QPD system then detects any potential instability such as cracks (Figure 3A). The QPD system measures the energy loss coefficient

(LC) and the software generates plots of data in the form of energy return graphs as a function of time in milliseconds (see Figure 4 for examples of energy return graphs).

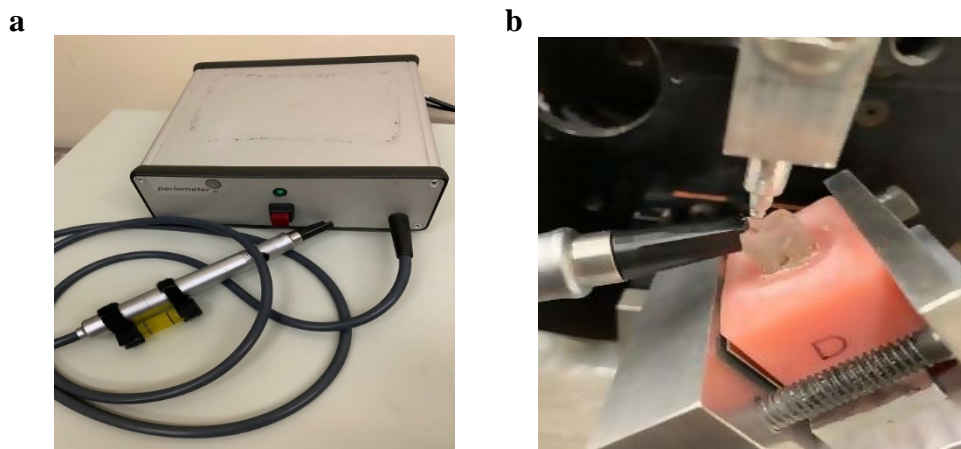


**Figure 3. Perimeter system a.** Main components of the machine includes percussion probe attached to a control unit. **b.** Testing of the simulated tooth (D-L cusp) using the Quantitative percussion diagnostics instrument. The probe is held perpendicular to the specimen for measurement.

#### Quantitative percussion testing of simulated teeth

Each of the 3D replica molar teeth were initially tested with QPD to ensure no cracks were present prior to the experiment. The data generated from QPD included two main characteristics: Normalized percussion energy return, loss coefficient (LC) as a function of time which measures overall tooth stability, and normal fit error (NFE) which indicates localized mobility due to a defect.<sup>17</sup>

Initially, the simulated tooth is tested to about 100k-120k cycles when normally a crack is introduced. After the crack is initiated, as soon as the NFE starts to increase rapidly, the tooth is mounted with the simulated periodontal ligament (Rubber Sep) and cortical bone (acrylic). The specimen is lowered on the fatigue machine to allow space for placement of the Perimeter handpiece tip on the cusps of the simulated tooth, in this case, the distal-lingual cusp (Figure 3B). The computer software is then started for the Perimeter testing of the specimen (Figure 4B).



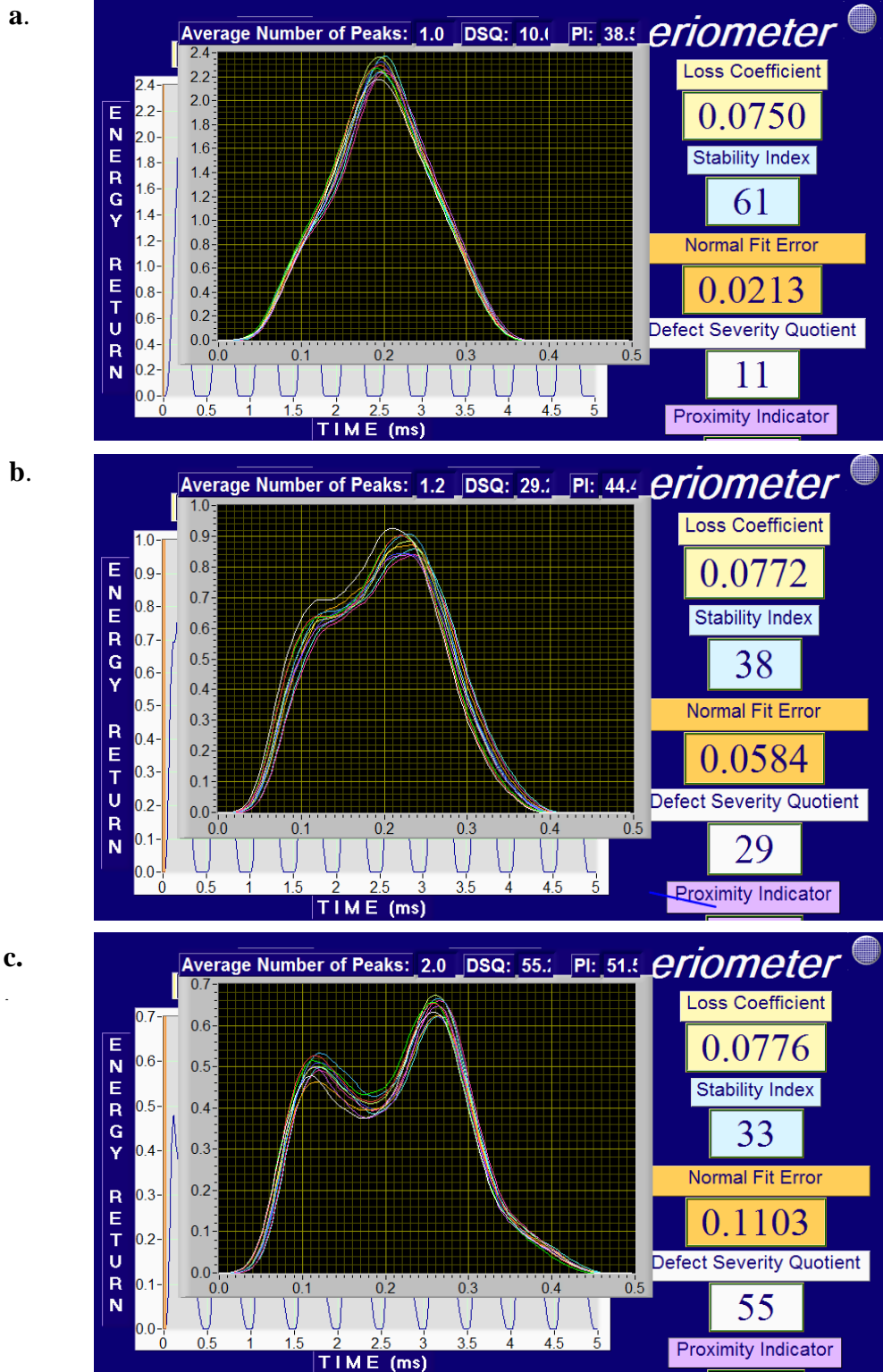


**Figure 4. QPD generated energy return graphs.** a. Normal curve without a crack as only one peak is present. Defect severity quotient (DSQ) of 20 to 50 indicates the presence of a potential minor crack. b. Presence of a minor peak in addition to the larger peak indicating the potential for a crack formation in the tooth. Greater than 50 DSQ indicates the potential for a crack initiation c. Presence of two peaks indicates the presence of a crack. Normal fit error (NFE) = DSQ/500

Once the name of the experiment is entered (e.g. For tooth 7.2, 7 is the tooth number and 2 refers to the second test after 20K on the fatigue machine), number of tests are then entered. The Perimeter percussion probe is subsequently placed on the desired cusp of the specimen making sure it remains horizontal (Figure 3B). The data is recorded for each of the replica teeth from 6 of these percussions and registered by the system software as the plot of energy versus time for each impact with an average taken for the NFE (Figure 4). The LC is determined from the recorded raw energy returns.

#### Measurement for NFE

Following each fatigue cyclic testing, the tooth sample is lowered to perform the QPD experiment. NFE is a difference between ideal single pick response and multiple pick response. The contact between crack phases during percussion makes NFE to increase. The NFE was measured from the Perimeter device. For each simulated tooth, QPD test was repeated five times and the maximum value of NFE was recorded accordingly.

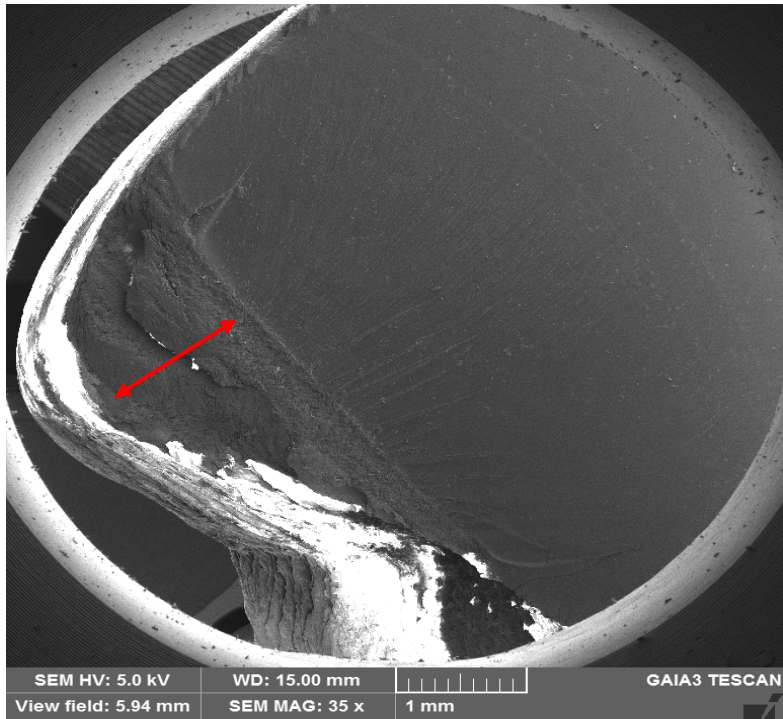
#### ***2.2.3 Fracture surface examination***

Following the fatigue test, the fracture surface was analyzed. Both the origin of crack, fracture mode and notches were identified. After mechanical testing we used a Scanning Electron Microscope (SEM) set at 34x to 35x magnification to evaluate properties of crack identified from the cross sections of sample teeth. Figure 5 illustrates an SEM of tooth no 9 notch depth and tooth no 4 crack properties including the position of the crack and distance the crack traveled along with the tooth.

### **2.3 Statistical analysis**

Statistical significance was determined by subjecting the data to Paired Samples t-test with significance set at  $P < 0.05$ .

a.



b.

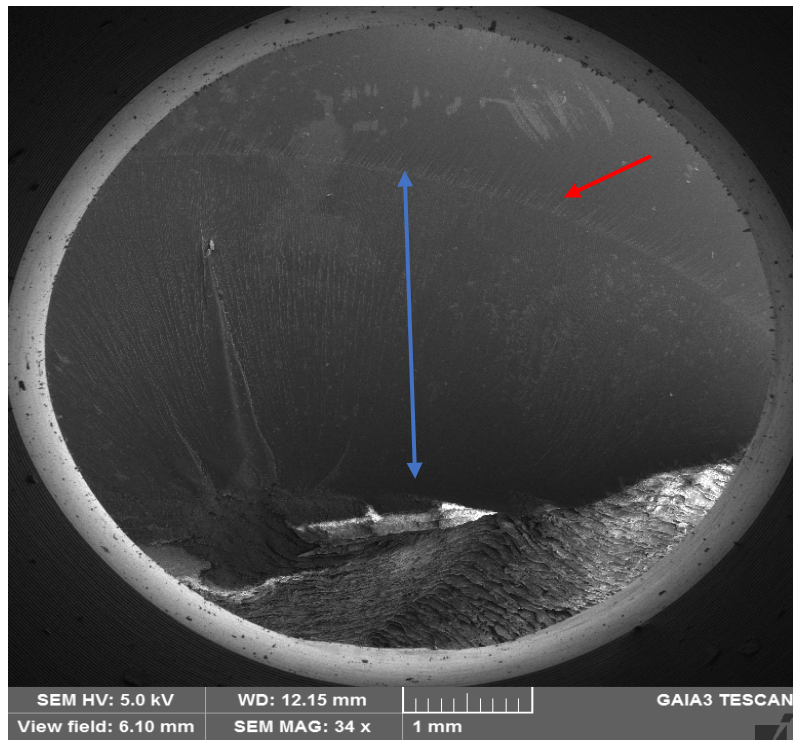


**Figure 5.. SEM of the Cross-section of 3D simulated teeth. a.** Tooth no. 9 notch position. The distance represented with the double head red arrow indicates the maximum distance of the notch depth measured for consistency at this depth. **b.** Tooth no 4 crack origin. The red line is at the border between fatigue crack and catastrophic fatigue. The blue line represents the fatigue crack distance.

## CHAPTER 3: Results & Discussion

### 3.1 Fatigue cycling and Crack initiation

#### 3.1.1 Summary of findings

Out of the nine specimens, a total of four specimens showed crack initiation in less than 200,000 cycles (Table 1) with one pilot specimen at more than one million cycles (Appendix A). The difference between the cycle number to failure in the pilot and experimental specimens was due to the lack of notch in pilot tooth versus notch placed on the occlusal surface of the experimentally simulated teeth. This indicates a specified notch depth and location on the 3D tooth model is one of the main factors in determining the cycles required to reach crack initiation.

**Table 1.** Crack detection within simulated 3D tooth specimens determined by QPD technology. All fatigue testing performed on D-L cusp with a load of 92 N used.

Specimen	Notch Depth (mm)	Initial NFE	Final NFE	Cycles to Crack initiation	Fracture Status	NFE (at crack initiation)	FC/FS (%)
4	0.42 mm	0.0265	NR	82k	CF	NR	38.1
5	0.36 mm	0.0247	NR	100k	CF	0.056	37.1
6	0.32 mm	0.0179	0.1202	134k	PF	0.0231	NR
7	0.26 mm	0.0245	0.1311	144k	CF	0.0311	36.7
8	>1 mm	0.0892	0.1157	~10k	PF	0.1030	NR
9	0.94 mm	0.0584	0.1009	~10k	CF	0.0584	43.9

**NFE:** normal fit error. **NR:** Not Recorded. **CF:** Complete Fracture; **PF:** Partial Fracture; **FS:** Fracture surface; **FC:** Fatigue Crack

An inverse relationship is apparent from the depth notch and cycles in comparison to the initiated crack. In other words, with an increase in the notch depth, the number of cycles of crack initiation tends to decrease as expected. In addition, with an increase in the notch depth,

the ratio of fatigue crack per fracture surface length tends to increase concomitantly. This relationship will further our understanding of both fatigue and catastrophic cracks. The load data for simulated 3D teeth are presented in Appendix A. Pairwise comparison of the NFE values for a tooth no. 6 and 7 revealed no statistical significance ( $p= 0.099$ ). See Table 2.

**Table 2.** Paired Samples Statistics for 3D tooth numbers 6 and 7

		Mean	S.D	N	95% Confidence Interval		t	df	Sig (2-tailed)
					Lower	Upper			
Pair	Six	0.0305	0.0167	30					
	Seven	0.0353	0.0263	30					
Paired differences		0.0048	0.0153	-	-0.0104	0.0009	-1.71	29	0.099

### ***3.1.2 Pilot fatigue testing of simulated teeth***

We were able to initiate a microcrack in nearly all simulated teeth except two while keeping the integrity of the tooth intact. The no. 3 simulated tooth was used for pilot testing of the M-L and M-B cusps (See Figure 6). While the M-L cusp showed cracking after one million cycles, the crack was evident in the M-B cusp after application of only 105K cycles. The initiated crack for the M-L cusp was in a vertical direction with only the coronal part of the tooth fractured. For the M-B cusp, the initiated crack was horizontal along the junction of the crown and root parallel to the occlusal plane (Figure 6A). The reason for the horizontal crack on M-B cusp is possibly due to the wider M-B cusp structure.

### ***3.1.3 Experimental fatigue testing of simulated 3D teeth***

For the experimental simulated teeth no. 4 to 9 a single notch of about 0.25 to 1 mm was created in the occlusal plane where all the cusps met at the center of the tooth. The notch placement was to allow for more flexibility in the simulated tooth structure so as to lower the number of cycles required for microcrack formation (Figure 6B).

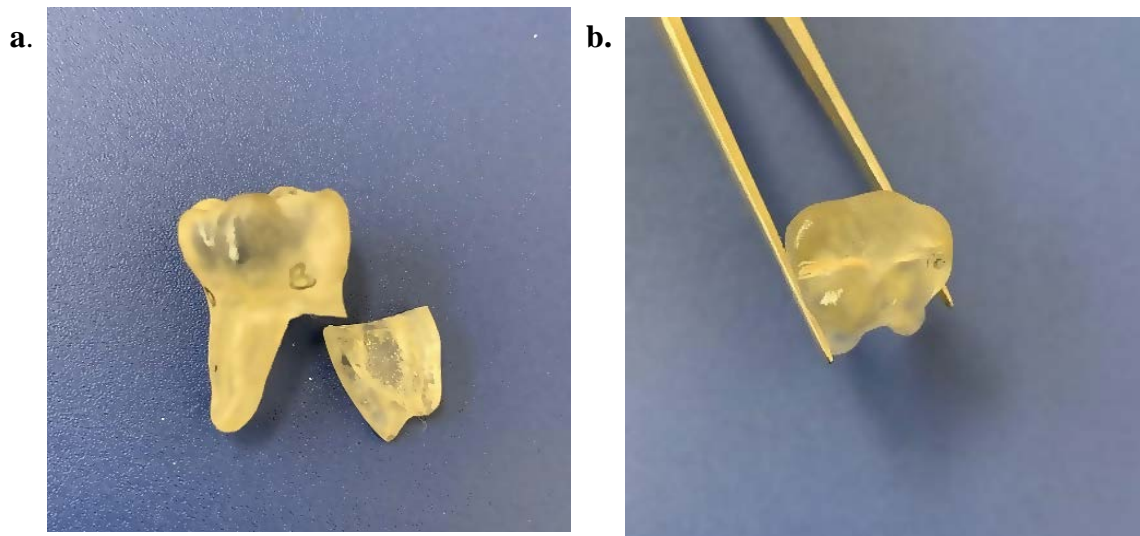


**Figure 6. Examples of simulated teeth. a.** Fatigue tested horizontally fractured M-B cusp at root and crown junction. **b.** Example of a central notch created on the occlusal surface of an experimental simulated tooth.

The fatigue test for tooth no. 4 (0.42 mm notch) was performed on the D-L cusp which showed a vertical crack formation after 82K cycles (Figure 7A). As expected, the notch accelerated crack initiation on the D-L cusp. The notch on tooth no.4 was deeper than other teeth creating more flexibility and bending moments, hence initiating crack the fastest.

The notch on tooth no.5 was 0.36 mm, and crack initiation occurred after 100K cycles on the D-L cusp in a vertical direction (Figure 7B). Due to errors introduced in data collection for tooth no.5, the results are excluded for analysis. Therefore, a crack is formed nearly after 100K cycles when testing is done on the D-L cusp of the simulated teeth.

The fatigue testing on the D-L cusp of tooth no.6 revealed a significantly high number of defect severity quotients (~ 40) but no crack was initiated. As a result, we did not continue with inducing crack initiation in this tooth. Instead, a fixed tooth holder will be used in order to simulate real conditions for future testing. In addition, the location of the pin may have hindered the detection of a crack in this simulated tooth model. The location of the pin for this tooth was more central which translates to a longer time for the crack to be initiated.

This result is also supported by the presence of less bending moment near the center of the tooth than the cusps. The graph in Figure 8A shows that at around 134K cycles (red arrow) there is the start of exponential growth with a potential crack initiating. However, we halted this experiment at this point because we wish to use tooth no. 6 for further studies.

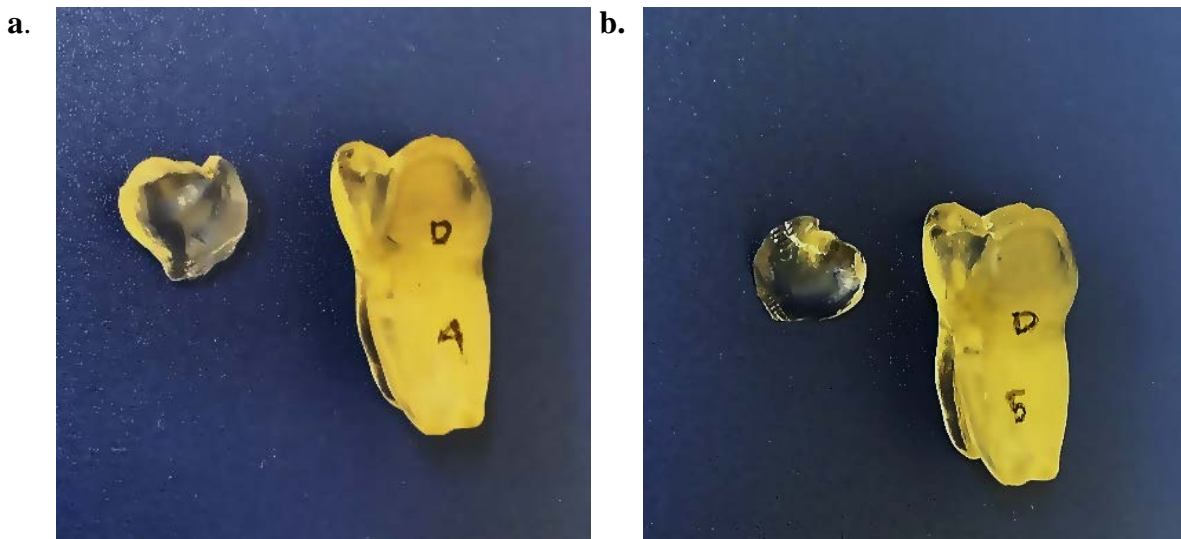


**Figure 7. Fatigue test in experimental simulated models. a.** Tooth no. 4 vertical fracture along the D-L cusp after 82K cycles. **b.** Tooth no. 5 vertical fracture after 118K cycles.

For fatigue testing of tooth no.7 on the D-L cusp, we applied the changes after tooth no.6 simulation, namely using a fixed tooth holder at around 170k cycles as we noticed the high number of NFE indicating minor crack initiation. The graph for tooth no. 7 (Figure 8B) shows a potential crack initiation at nearly 144K cycles (red arrow) after which there is exponential growth. At around 208K cycles a vertical crack on the D-L cusp is detected with partial fracture of the crown. The fatigue testing for tooth no.8 was not completed due to the experimental error of creating a very deep notch on the sample, hence excluded from results.

Fatigue testing of tooth no.9 did not reveal a crack initiation as the depth of notch (0.94 mm) was slightly higher than the other experimental teeth. This resulted in the occurrence of a crack at a much faster rate and we were unable to detect the crack initiation. From the graph in Figure

8C, it appears that the crack may have initiated after 10K cycles and completed at about 55K cycles. These experiments highlight the importance of notch creation and require careful planning for future experiments. For teeth no. 3 an R ratio of 0.1 was used and we found that this ratio will take at least a million cycles thereby hindering any detection of the crack initiation. Consequently, we changed the R ratio to 0.2 for teeth no. 4 to 9 as this allowed us to detect the crack just before it occurs by reducing the testing time. Both teeth no. 6 and 8 survived the fatigue cyclic test and will be used for future experiments.

### **3.2 Significance of findings and clinical implications**

We conducted fatigue cycling testing of 3D simulated teeth using QPD technology to detect potential crack initiation. This study adds to the growing literature on the mechanism of fatigue cycling. Furthermore, this research may lead to the development of powerful tools integrating QPD technology that potentially can become routine in clinical examination procedures to monitor teeth structural integrity. QPD device can also serve as a motivational tool for patient education and preventive treatment planning to improve the long-term life of teeth and restorations.<sup>18</sup>

### **3.3 Limitations of the study**

One of the main limitations of this study was that challenges of the oral environment which could not be closely simulated in the *in vitro* setting. One of the causes of tooth material failure is repeated changes in pH of the oral environment which leads to corrosive pit formation,<sup>19,20</sup> and reduced fatigue life during the crack growth on the surface of a dental implant. There are a few technical considerations to be made for future studies. The 3D tooth models need to be mounted standard to ensure uniform orientation among the specimens. The testing load needs to be re-evaluated to ensure more tooth failures occur and that it is clinically relevant. The conclusions made here are based on the analysis of only a few simulated tooth models, therefore



additional teeth are required to confirm these findings. As we only used simulated 3D tooth models, it is important to compare these findings with testing done in natural extracted teeth. In addition, the QPD data should be compared to transillumination testing and dye penetrant to simulate clinical setting. The most important step is to design conditions that allow translation of *in vitro* results to clinically failed dental materials (e.g. implants) and thus validate the testing process.

### **3.4 Conclusions and Future directions**

In the present study cyclic fatigue and crack, the detection was studied by simulating natural biomechanical forces on a 3 D tooth model using the QPD technology. The preliminary results obtained for molar 3D simulated teeth show that cyclic loading of the D-L cusp resulting in failure stress and eventual vertical fracture of the tooth was detected by the QPD device. Design of notch on the occlusal surface of the tooth influenced time to reach crack initiation. Despite preliminary, these *in vitro* results are promising and provide motivation to improve the methodology and optimize testing parameters for detection of crack initiation using the QPD device.

Since we only performed fatigue testing on the D-L cusp, future experiments will be focused on testing M-B and M-L cusps to determine the cycles and time required for crack initiation. Moreover, since fixed holder simulates oral environment it will be used in future experiments. We will also carefully plan the location and depth of notch on the occlusal surface of the simulated teeth since it was found that notch placement plays an important role in identifying the number of cycles needed for crack initiation and subsequent growth process.

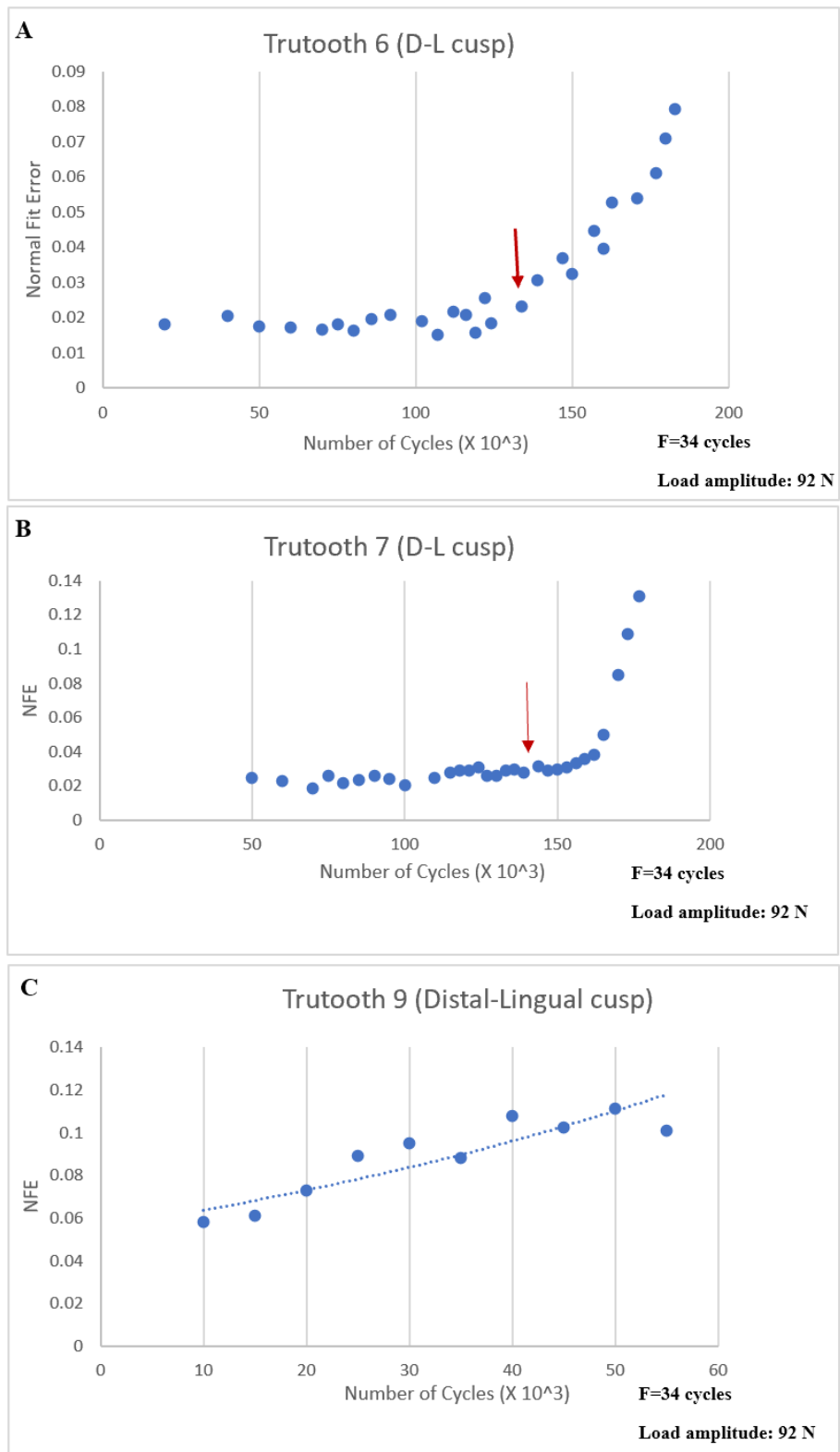


**Figure 8. Fatigue testing.** Plot of NFE versus cycles to failure for **a.** tooth no. 6.; **b.** tooth no. 7; **c.** tooth no. 9. Red arrow indicates the approximate cycle that crack was initiated

## REFERENCES

1. Arola D, Bajaj D, Ivancik J, Majd H, Zhang D. fatigue of biomaterials: hard tissues. *International journal of fatigue*. 2010;32(9):1400-1412.
2. Kruzic J, Ritchie R. Kitagawa-Takahashi diagrams define the limiting conditions for cyclic fatigue failure in human dentin. *Journal of Biomedical Materials Research Part A: An Official Journal of The Society for Biomaterials, The Japanese Society for Biomaterials, and The Australian Society for Biomaterials and the Korean Society for Biomaterials*. 2006;79(3):747-751.
3. Lawn BR, Lee JJ. Analysis of fracture and deformation modes in teeth subjected to occlusal loading. *Acta Biomaterialia*. 2009;5(6):2213-2221.
4. Yahyazadehfar M, Ivancik J, Majd H, An B, Zhang D, Arola D. On the Mechanics of Fatigue and Fracture in Teeth. *Applied mechanics reviews*. 2014;66(3):0308031-3080319.
5. Arola DD, Gao S, Zhang H, Masri R. The Tooth: Its Structure and Properties. *Dental clinics of North America*. 2017;61(4):651-668.
6. Zhang Y-R, Du W, Zhou X-D, Yu H-Y. Review of research on the mechanical properties of the human tooth. *International Journal Of Oral Science*. 2014;6:61.
7. Bajaj D, Nazari A, Eidelman N, Arola DD. A comparison of fatigue crack growth in human enamel and hydroxyapatite. *Biomaterials*. 2008;29(36):4847-4854.
8. Imbeni V, Kruzic J, Marshall G, Marshall S, Ritchie R. The dentin-enamel junction and the fracture of human teeth. *Nature materials*. 2005;4(3):229.
9. Ruse N, Troczynski T, MacEntee M, Feduik D. Novel fracture toughness test using a notchless triangular prism (NTP) specimen. *Journal of Biomedical Materials Research: An Official Journal of The Society for Biomaterials and The Japanese Society for Biomaterials*. 1996;31(4):457-463.

10. Zhang D, Nazari A, Soappman M, Bajaj D, Arola D. Methods for examining the fatigue and fracture behavior of hard tissues. *Experimental Mechanics*. 2007;47(3):325-336.
11. Mathew S, Thangavel B, Mathew CA, Kailasam S, Kumaravadivel K, Das A. Diagnosis of cracked tooth syndrome. *Journal of pharmacy & bioallied sciences*. 2012;4(Suppl 2):S242-S244.
12. Clark DJ, Sheets CG, Paquette JM. Definitive diagnosis of early enamel and dentin cracks based on microscopic evaluation. *Journal of esthetic and restorative dentistry : official publication of the American Academy of Esthetic Dentistry [et al]*. 2003;15(7):391-401; discussion 401.
13. Culjat MO, Singh RS, Brown ER, Neurgaonkar RR, Yoon DC, White SN. Ultrasound crack detection in a simulated human tooth. *Dento maxillo facial radiology*. 2005;34(2):80-85.
14. Fried WA, Simon JC, Lucas S, et al. Near-IR imaging of cracks in teeth. *Proceedings of SPIE--the International Society for Optical Engineering*. 2014;8929:89290Q-89290Q.
15. Stanley B, Bustemante L, Earthman J. "Novel instrumentation for rapid assessment of internal damage in composite materials." *Nondestructive Evaluation and Materials Properties III (1997)*. 1997.
16. Brenner D, Earthman J. Novel instrumentation for quantitative determination of energy damping in materials and structures. *Scripta metallurgica et materialia*. 1994;31:467-471.
17. Sheets CG, Stewart DL, Wu JC, Earthman JC. An in vitro comparison of quantitative percussion diagnostics with a standard technique for determining the presence of cracks in natural teeth. *The Journal of prosthetic dentistry*. 2014;112(2):267-275.
18. Sheets CG, Wu JC, Earthman JC. Quantitative percussion diagnostics as an indicator of the level of the structural pathology of teeth: Retrospective follow-up investigation of

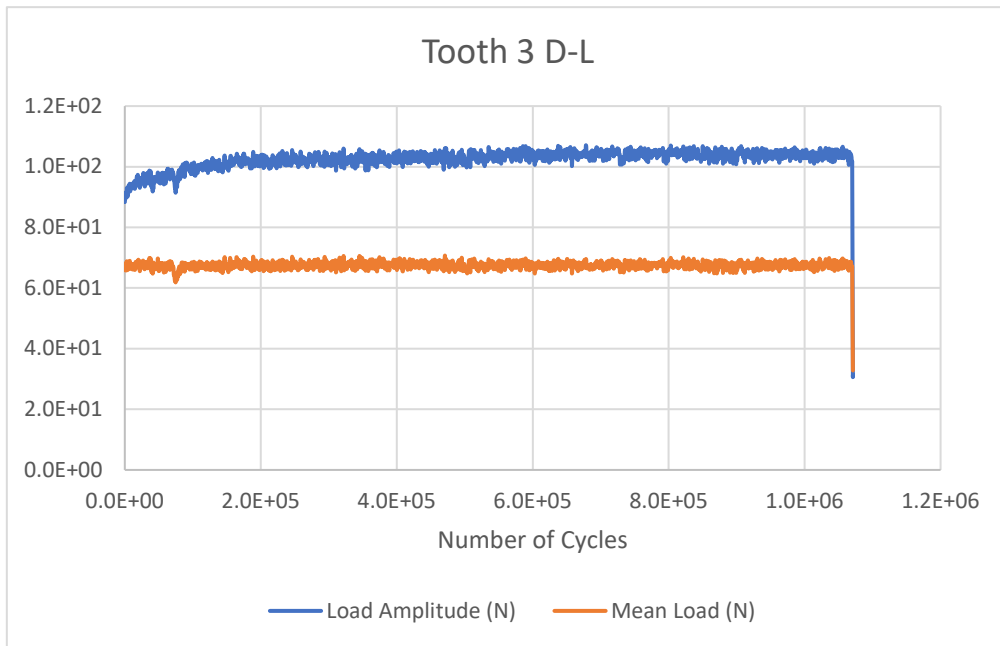
high-risk sites that remained pathological after restorative treatment. *The Journal of prosthetic dentistry*. 2018;119(6):928-934.

19. Huang H-M, Tsai C-M, Chang C-C, Lin C-T, Lee S-Y. Evaluation of loading conditions on fatigue-failed implants by fracture surface analysis. *International Journal of Oral & Maxillofacial Implants*. 2005;20(6).

20. Piattelli A, Scarano A, Paolantonio M, et al. Fluids and microbial penetration in the internal part of cement-retained versus screw-retained implant-abutment connections. *Journal of periodontology*. 2001;72(9):1146-1150.

## APPENDIX A: Load data for simulated 3D teeth

A.



B.

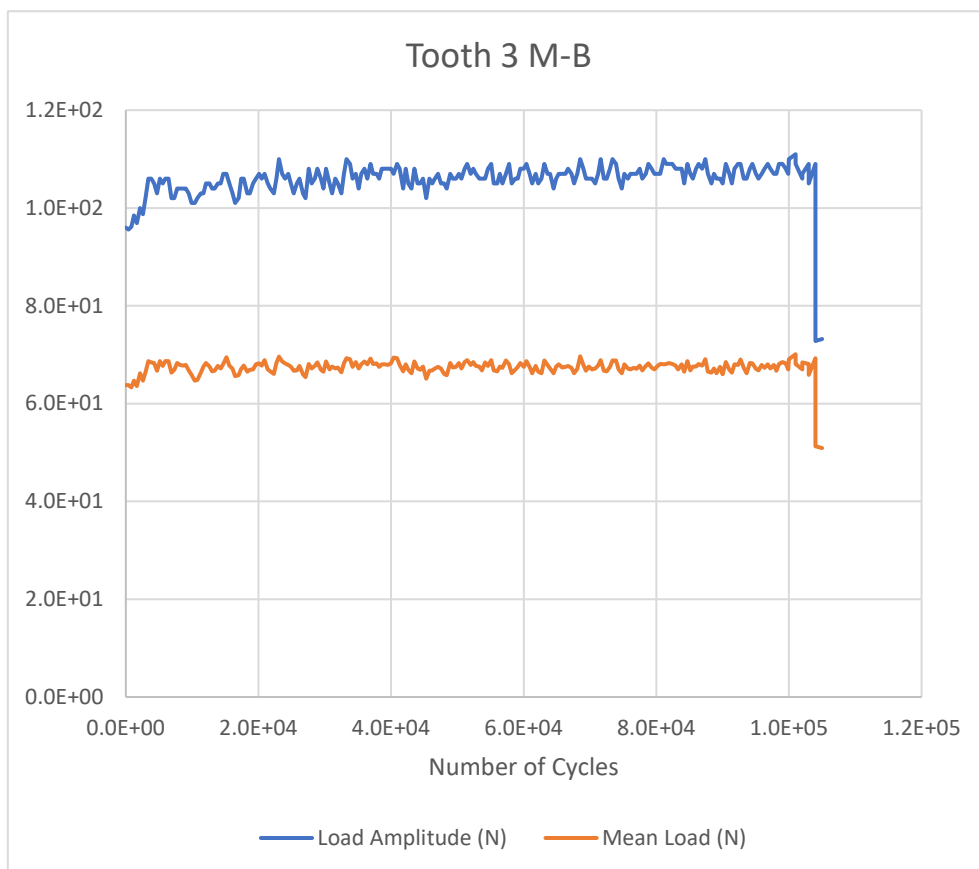
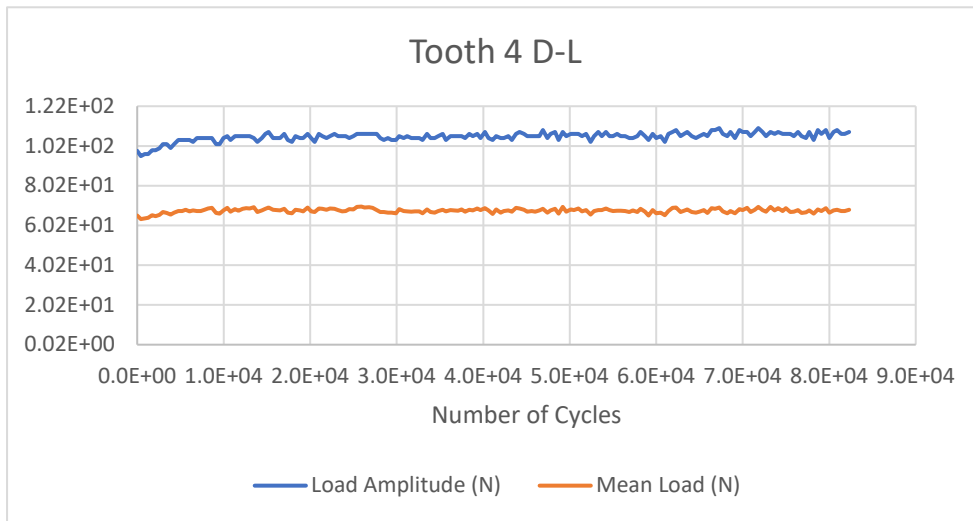
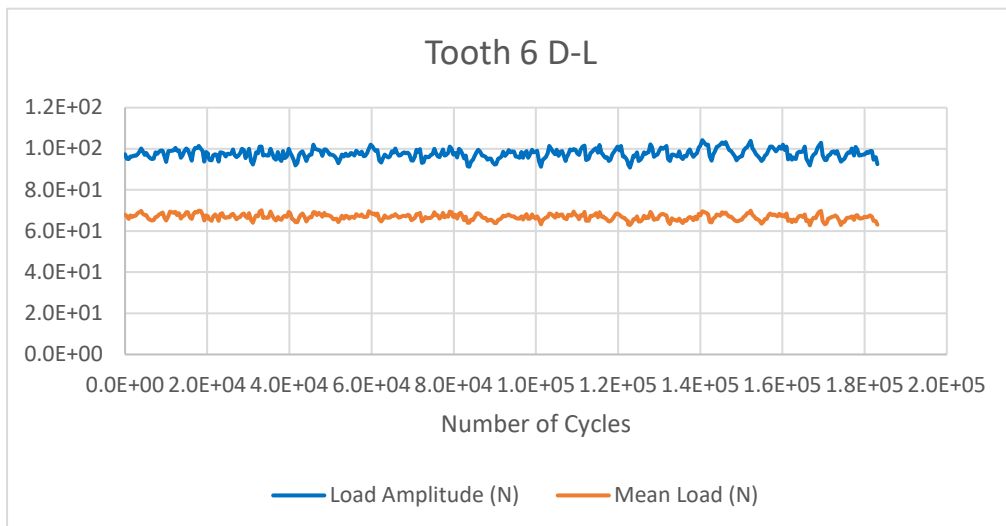


Figure A.1 Graph of Load versus cycle number for simulated tooth number 3, A. D-L; B.M-B cusp

**A.**



**B.**



**C.**

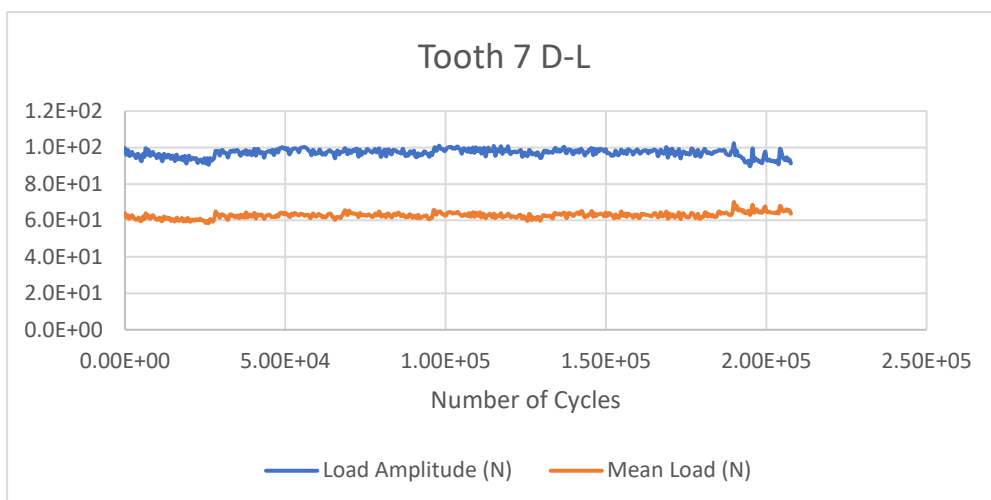


**Figure A2.** Graph of Load versus cycle number for simulated tooth number 4,6 and 7

## APPENDIX B: Fatigue Testing Procedure

### Preparation of Samples:

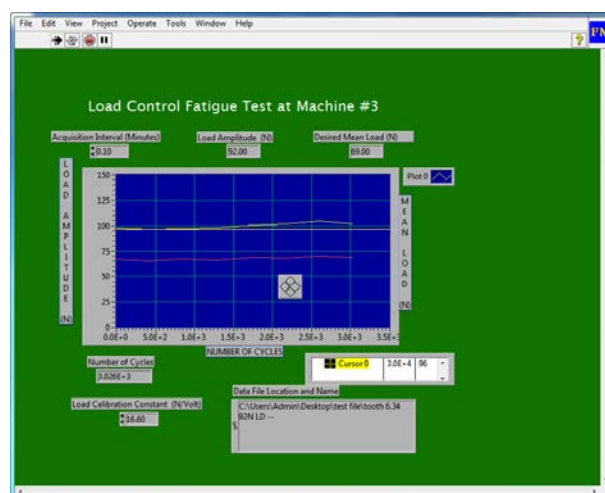
- Samples are prepared by securing in an acrylic-based separable simulated cortical bone
- Location of acrylic adjusted to have desired distance between the tooth cusp and locator pin

### Steps to prepare Software parameters:

- Open Custom LabView VI and Select Newport ESP301 then select OK

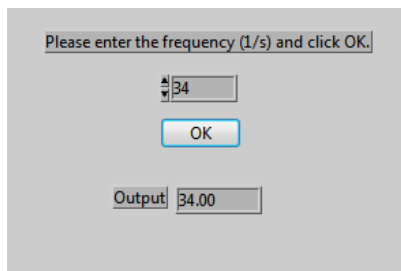


- On the main Window click on Run button on the top left corner





- Enter the frequency of 34 cycles per second then click on OK



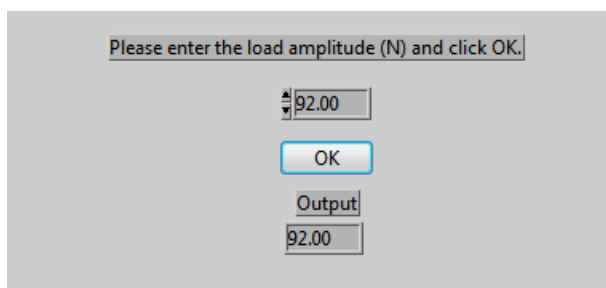
Please enter the frequency (1/s) and click OK.

34

OK

Output: 34.00

- Enter Load Amplitude of 92 N and Click OK



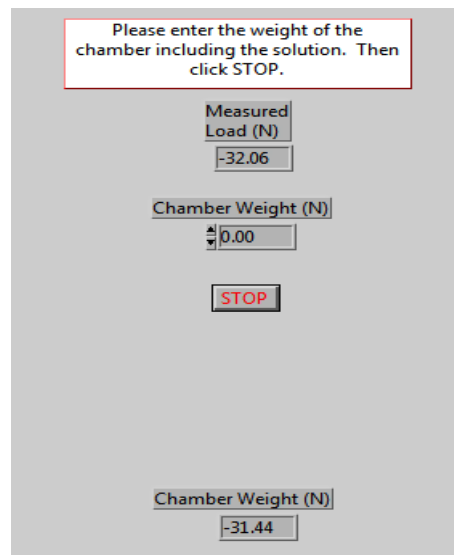
Please enter the load amplitude (N) and click OK.

92.00

OK

Output: 92.00

- Enter the weight of the chamber of -32N which make the overall weight zero and then press and hold Stop for 3 seconds



Please enter the weight of the chamber including the solution. Then click STOP.

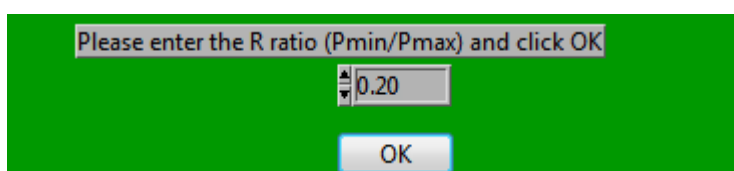
Measured Load (N)  
-32.06

Chamber Weight (N)  
0.00

STOP

Chamber Weight (N)  
-31.44

-Enter the value for R Ratio ( $P_{Min}/ P_{Max}$ ) then click Ok

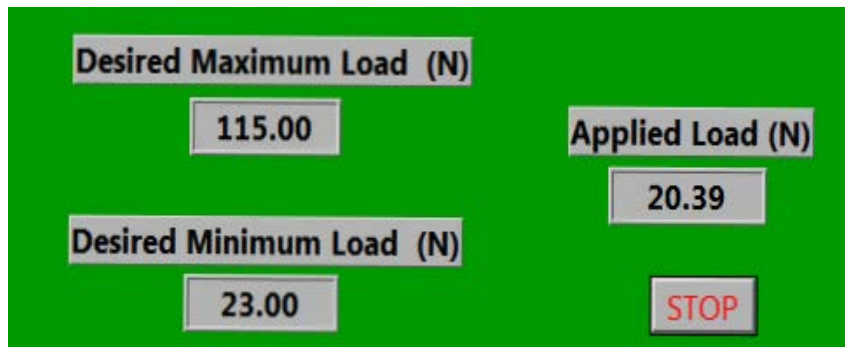


Please enter the R ratio (Pmin/Pmax) and click OK

0.20

OK

-Adjust the Load until it equals the Desired Load showed below and press and hold the Stop button for 5 second



- Save the file in the desired location

**Note:** This process was performed repeatedly every 10k cycles up to 70k cycles, then every 5k cycles up to 120k and every 3k cycles until major changes on NFE value were observed.